Journal of Photochemistry and Photobiology B: Biology 117 (2012) 27–32

Contents lists available at SciVerse ScienceDirect

Journal of Photochemistry and Photobiology B: Biology

journal homepage: www.elsevier.com/locate/jphotobiol

Docking investigation and binding interaction of benzimidazole derivative with bovine serum albumin

J. Jayabharathi *, K. Jayamoorthy, V. Thanikachalam

Department of Chemistry, Annamalai University, Annamalainagar 608 002, Tamilnadu, India

ARTICLE INFO

Article history:
Received 25 July 2012
Received in revised form 21 August 2012
Accepted 27 August 2012
Available online 5 September 2012

Keywords:
Benzimidazole
Molecular docking
BSA
Quenching

ABSTRACT

^{1}H NMR, ^{13}C NMR and Mass spectral analysis have been made for 1-(4-fluorobenzyl)-2-(4-fluorophenyl)-1H-benzo[d]imidazole (FBFPB). The mutual interaction of FBFPB with bovine serum albumin (BSA) was investigated using absorption, fluorescence and synchronous fluorescence spectral studies. The binding distance has been determined based on the theory of Forester's non-radiation energy transfer (FRET). The calculated quenching constants (K_{sv}) were 2.84×10^4, 2.55×10^4 and 2.37×10^4 at 301, 310 and 318 K respectively. The Stern–Volmer quenching constant (K_{sv}), binding site number (n), apparent binding constant (K_A) and corresponding thermodynamic parameters (ΔG, ΔH and ΔS) were calculated. The interaction between FBFPB and BSA have discussed by molecular docking technique.

1. Introduction

Heterocyclic imidazole derivatives have attracted considerable attention because of their unique optical properties [1] and used for preparing functionalized materials [2]. Imidazole nucleus forms the main structure of human organisms, i.e., the amino acid histidine, Vitamin B_{12}, a component of DNA base structure and also has significant analytical applications utilizing their fluorescence and chemiluminescence properties [3,4].

BSA is made up of three homologous domains (I–III), which are divided into nine loops by 17 disulfide bridges. Each domain is composed of two sub-domains (A and B). Aromatic and heterocyclic ligands were found to bind within two hydrophobic pockets in sub-domain IIA and IIIA, site I and site II [5,6]. BSA has two tryptophans, Trp-134 and Trp-212, embedded in the first sub domain IB and sub-domain IIA, respectively. There is evidence of conformation changes of BSA induced by its interaction with low molecular weight benzimidazole and imidazole ligands [7–10]. It is important to study the interaction of FBFPB with BSA, and hence become an important research field in chemistry, life sciences and clinical medicine. The molecular structure of FBFPB is given in Fig. 1. In the present research article, we have studied the binding interaction of BSA with 1-(4-fluorobenzyl)-2-(4-fluorophenyl)-1H-benzo[d] imidazole.

2. Experimental

2.1. Materials and methods

All BSA solution were prepared in the Tris–HCl buffer solution (0.05 mol L^{-1} Tris, 0.15 mol L^{-1} NaCl, pH 7.4) and it was kept in the dark at 303 K. Tris base (2-amino-2-(hydroxymethyl)-1,3-propanediol) had a purity of not less than 99.5% and NaCl, HCl and other starting materials were all of analytical purity and doubly distilled water was used throughout.

2.2. Optical measurements

NMR spectra have been recorded for the FBFPB on a Bruker 400 MHz instrument. The ultraviolet–visible (UV–vis) spectra have been measured on UV–Vis spectrophotometer (Perkin Elmer, Lambda 35) and corrected for background due to solvent absorption. Photoluminescence (PL) spectra have been recorded on a (Perkin Elmer LS55) fluorescence spectrometer. Solvents used for spectral measurements are spectroscopic grade. Mass spectra have also been recorded on a Varian Saturn 2200 GCMS spectrometer.

2.3. Molecular docking

The rigid molecular docking studies were performed by using HEX 6.1 software [11], is an interactive molecular graphics program to understand the drug-protein interaction. The Structure of the FBFPB was sketched by CHEMSKETCH (http://www.acdlabs.com) and converts it into pdb format from mol format by OPENBABEL (http://www.vcclab.org/lab/babel/). The crystal

* Corresponding author. Tel.: +91 9443940735.
E-mail address: jtchalam2005@yahoo.co.in (J. Jayabharathi).

1011-1344/$ - see front matter © 2012 Elsevier B.V. All rights reserved.
http://dx.doi.org/10.1016/j.jphotobiol.2012.08.018

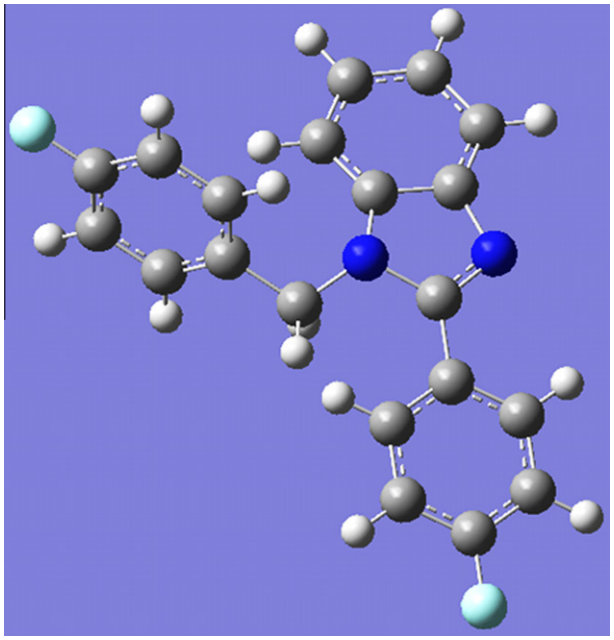

Fig. 1. Molecular structure of FBFPB.

structure of HSA (PDB entry 1AO6) is obtained from the Protein Data Bank (http://www.rcsb.org./pdb). Since the structure of bovine serum albumin (BSA) is unavailable in the PDB, a homology model was used for the docking studies. All calculations were carried out on an Intel pentium 4, 2.4 GHz based machine running MS Windows XP SP2 as operating system. Visualization of the docked pose has been done by using PyMol (http://pymol.sourceforge.net/) molecular graphic program.

2.4. General procedure for the synthesis of ligands

A mixture of 4-fluorobenzaldehyde (2 mmol), *o*-phenylenediamine (1 mmol) and ammonium acetate (2.5 mmol) has been refluxed at 80 °C in ethanol. The reaction was monitored by TLC and purified by column chromatography using petroleum ether: ethyl acetate (9:1) as the eluent.

2.4.1. 1-(4-Fluorobenzyl)-2-(4-fluorophenyl)-1H-benzo[d]imidazole

Yield: 55%. mp = 84 °C, Anal. calcd. for $C_{20}H_{14}F_2N_2$: C, 74.98; H, 4.41; F,11.86; N, 8.75. Found: C, 74.49; H, 4.51; F,11.95; N, 9.05. ^{1}H NMR (400 MHz, $CDCl_3$): δ5.41 (s, 2H), 7.02–7.08 (m, 4H), 7.15–7.18 (t, 3H), 7.22–7.23 (d, 1H) 7.26–7.29 (m, 1H), 7.33–7.36 (m, 1H), 7.65–7.67 (m, 2H), 7.87–7.88 (s, 1H). ^{13}C (100 MHz, $CDCl_3$): δ 47.71 (–CH_2 carbon), 110.33, 115.93, 116.03, 116.21, 120.07, 122.92, 123.30, 126.16, 126.19, 127.60, 127.63, 127.67, 131.19, 131.25, 131.93, 131.95, 135.89, 143.06, 153.08, 161.31, 162.78, 163.28, 164.77 (Aromatic carbons). MS: *m/e* 320.1, calcd 321.11 [M + 1].

3. Results and discussion

3.1. Fluorescence spectral studies

The interaction between FBFPB and BSA was investigated by evaluating fluorescence intensity on the BSA before and after the addition of the FBFPB [10,12]. Here, the concentrations of BSA were stabilized at 1.0×10^{-5} mol L^{-1} and the concentration of FBFPB varied from 0 to 3.5×10^{-5} mol L^{-1} at increments of 0.5×10^{-5} mol L^{-1}. The effect of the FBFPB on BSA fluorescence intensity is shown in Fig. 2. The fluorescence intensity of BSA decreases progressively but the emission maximum did not move to shorter or longer wavelength, due to the interaction of FBFPB with BSA and quench its intrinsic fluorescence (*Trp-212*) [13], but there was no alteration in the local dielectric environment of BSA.

The quenching mechanism of FBFPB with BSA was probed using the Stern–Volmer equation [14], which can be applied to determine K_{sv} by linear regression from the Stern–Volmer plot of F_0/F against [FBFPB] (Fig. 3) at different temperatures. Table 1 summarizes the values of K_{sv} and K_A at different temperatures, which shows the values of Stern–Volmer quenching constant K_{sv} and K_A decreases with increase in temperature. According to the literature [15] for dynamic quenching, the maximum scatter collision quenching constant of various quenchers with the biopolymer is 2.0×10^{10} L mol^{-1} s^{-1} and the fluorescence lifetime of the biopolymer is 10^{-8} s. From Fig. 3, the values of K_{sv} and k_q ($=K_{sv}/\tau_0$) were calculated. The obtained values of k_q were larger than the limiting diffusion rate constant of the biomolecule (2.0×10^{10} L mol^{-1} s^{-1}), which indicate that the fluorescence quenching is caused by a specific interaction between BSA and FBFPB. Therefore, the quenching mechanism mainly arises from the formation of BSA–FBFPB complex rather than dynamic quenching. So it was implied that the static quenching was dominant in the system. From the plot of log[($F_0 - F$)/F] *vs* log[FBFPB], binding constants K_A and the number of binding sites '*n*' were calculated from the intercept and slope.

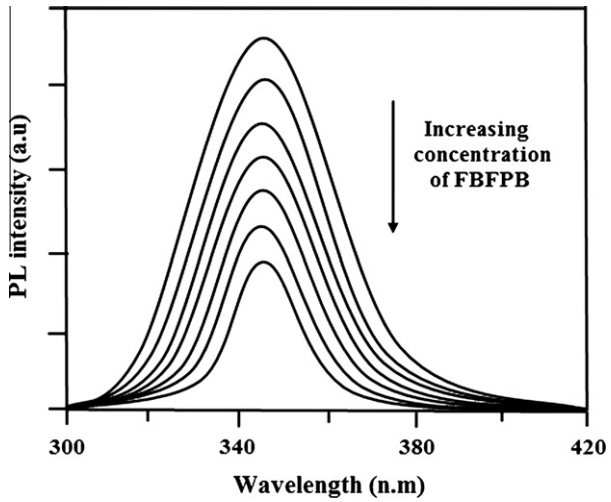

Fig. 2. Fluorescence quenching spectra of BSA at different concentrations of FBFPB.

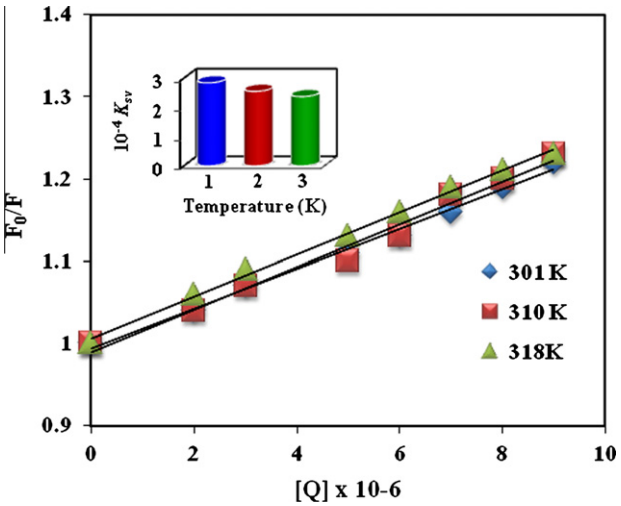

Fig. 3. Stern–Volmer plot of F_0/F against [FBFPB].

Table 1
K_{sv} K_A, n and r values of BSA–FBFPB system at 301, 310 and 318 K.

T (K)	K_{sv} (10^4 L Mol^{-1})	K_A (10^4 L Mol^{-1})	n	r
301	2.84	3.76	1.2	0.99
310	2.55	2.74	1.01	0.99
318	2.37	2.17	0.98	0.99

Table 2
Thermodynamic parameters of BSA–FBFPB system at 301, 310 and 318 K.

T (K)	ΔH (kJ mol^{-1})	ΔG (kJ mol^{-1})	ΔS (J mol^{-1}K^{-1})
301	−25.77	−24.55	1.88
310		−25.7	
318		−24.1	

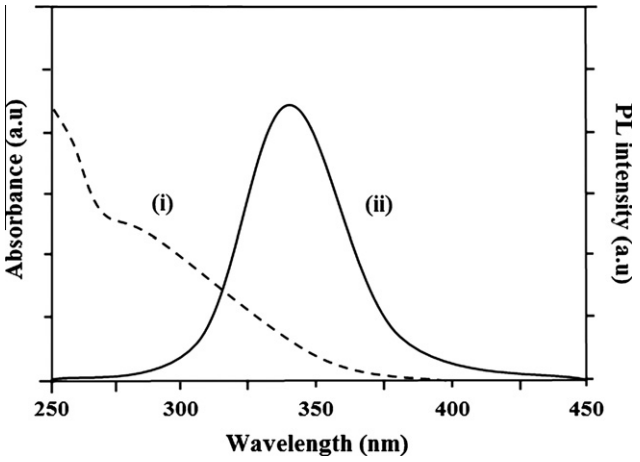

Fig. 4. Overlapping spectra of absorption (i) and emission (ii) of BSA with FBFPB.

3.2. Determination of thermodynamic parameters

In order to elucidate the interaction between the FBFPB and BSA, the thermodynamic parameters were calculated from the van't Hoff plots. If the enthalpy change (ΔH) does not vary significantly over the temperature range studied then the thermodynamic parameters ΔH, ΔG and ΔS can be determined from the following equations, respectively.

$$\ln K = \Delta H/RT + \Delta S/R \quad (1)$$

$$\Delta G = -RT \ln K \quad (2)$$

$$\Delta S = (\Delta H - \Delta G)/T \quad (3)$$

According to the theory of Ross, the positive enthalpy change (ΔH) and entropy change (ΔS) are associated with hydrophobic interaction. The negative values of ΔH and ΔS are associated with hydrogen binding and van der Waals interactions whereas the very low positive or negative ΔH and positive ΔS values are characterized by electrostatic interactions, From the Table 2 ΔH (−25.77), ΔG (−24.55) and ΔS (1.88), it was found that there is electrostatic interaction between BSA and FBFPB [16].

3.3. Energy transfer from BSA to FBFPB

Energy transfer takes place through direct electro-dynamic interaction between the excited molecule and its neighbours [17]. The distance between the donor (BSA) and the acceptor (FBFPB) was estimated by Forster's non-radiative energy transfer theory and the overlapping of fluorescence spectra of BSA with absorption spectra of FBFPB was shown in Fig. 4. According to Forster's non-radiative energy transfer theory, the energy transfer efficiency (E) can be defined as the following equations:

$$E = 1 - (F/F_0) = R_0^6/\left(R_0^6 + r_0^6\right) \quad (4)$$

$$R_0^6 = 8.8 \times 10^{-25}[k^2 n^{-4} \Phi_D J(\lambda)] \quad \text{in A}^\circ \quad (5)$$

$$J(\lambda) = \int_0^\infty F_D(\lambda)\varepsilon_A(\lambda)\lambda^4 d\lambda \quad (6)$$

where E is the efficiency of transfer between the donor and the acceptor, R_0 is the critical distance when the efficiency of transfer is 50%. $F_D(\lambda)$ is the corrected fluorescence intensity of the donor at wavelength λ to $(\lambda + \Delta\lambda)$, with the total intensity normalized to unity and $\varepsilon_A(\lambda)$ is the molar extinction coefficient of the acceptor at wavelength λ. The Forster distance (R_0) has been calculated assuming random orientation of the donor and acceptor molecules. Here, $k^2 = 2/3$, $n = 1.311$, $\Phi_D = 0.20$ and from the available data, it results that $J(\lambda) = 4.03 \times 10^{-12}$ cm^3 L mol^{-1}, $E = 0.34$, $R_0 = 0.73$ nm and $r = 0.79$ nm. The donor-to-acceptor distance is less than 8 nm which indicates that the energy could transfer from BSA to FBFPB [18] with high probability and the distance obtained by FRET with higher accuracy.

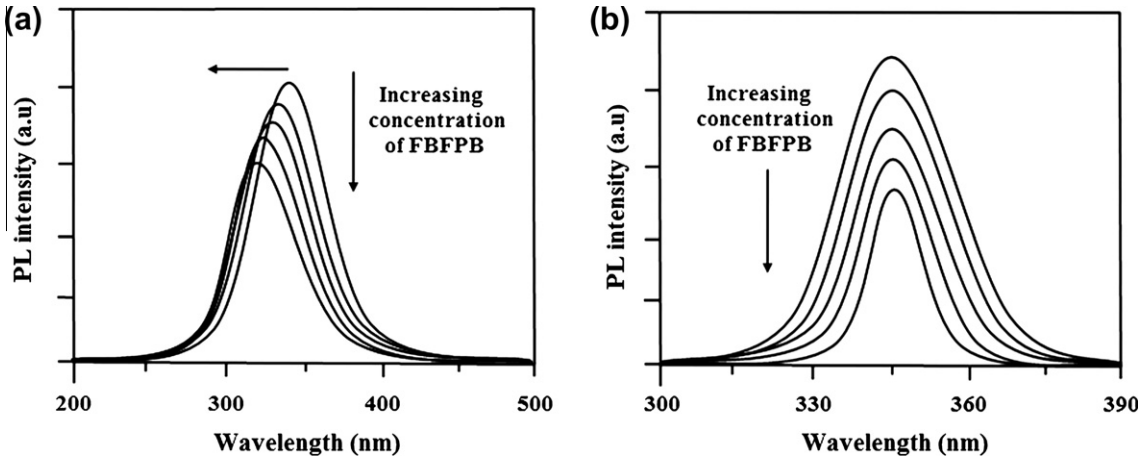

Fig. 5. Synchronous fluorescence spectra of BSA in the presence and absence of FBFPB (a) at $\Delta\lambda$ = 15 nm and (b) at $\Delta\lambda$ = 60 nm.

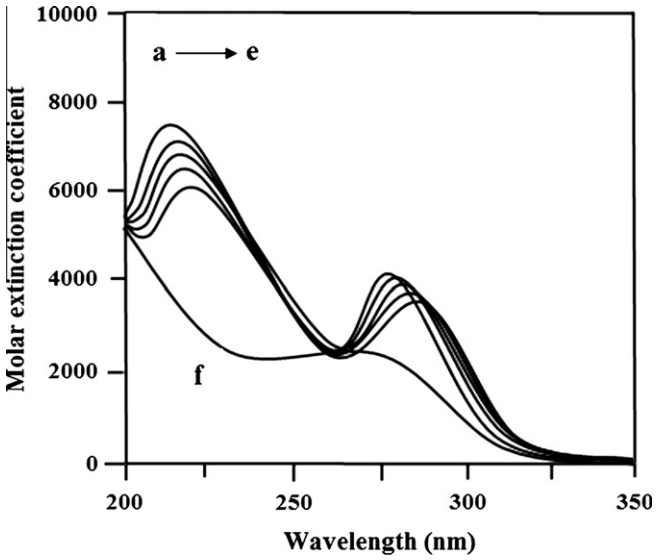

Fig. 6. Absorption spectra of BSA in the presence of FBFPB (a–e) and in the absence of FBFPB (f).

3.4. Conformation investigation

To exploit the structural change of BSA by addition of the FBFPB, we have measured synchronous fluorescence spectra of BSA with various amounts of FBFPB. The synchronous fluorescence spectra [12,19,20] of BSA with various amount of FBFPB were recorded at $\Delta\lambda = 15$ nm and $\Delta\lambda = 60$ nm (Fig. 5a and b). It is apparent from the figure that the emission wavelength of the tyrosine residues is blue-shifted (λ_{max} from 345 to 330 nm in Fig. 5a) with increasing concentration of FBFPB. This blue shift expressed that the conformation of BSA was changed and it suggested a less polar (or more hydrophobic) environment of tyrosine residue [21]. At the same time, the tryptophan fluorescence emission is decreased regularly, but no significant change in wavelength was observed. It suggests that the interaction of FBFPB with BSA does not affect the conformation of tryptophan micro-region. The tyrosine fluorescence spectrum may represent that the conformation of BSA is somewhat changed, due to the blue shift (Fig. 5a), leading to the polarity around *Tyr* residues was decreased and the hydrophobicity was increased [22], but the interaction of FBFPB with BSA does not obviously affect the conformation of tryptophan micro-region [23,24]. The FBFPB could involve the second site (sub-domain IB) with higher binding affinity and the formation of complex led to the observation of the blue shift of tyrosine residues fluorescence. This is because the tyrosine contains one aromatic hydroxyl group unlike tryptophan and tyrosine can undergo an excited state ionization, resulting in the loss of the proton on the aromatic hydroxyl group. The hydroxyl group can dissociate during the lifetime of its excited state, leading to quenching. Hence the aromatic hydroxyl group present in the tyrosine residues is responsible for the interaction of BSA with FBFPB.

For reconfirming the structural change of BSA by the addition of the FBFPB, we have measured the UV–vis absorbance spectra of BSA with various amounts of the FBFPB. Fig. 6 displays the UV–vis absorbance spectra of BSA at different concentrations of the FBFPB. The absorption band of 210 nm of BSA is characteristic of α-helix structure of BSA. The intensity of absorbance of BSA was decreased with increasing concentration of the FBFPB and the peak was red shifted. In addition, the absorption peaks in the UV–vis spectra at approximately 280 nm rise gradually (from curve (a) to curve (e)) and blue shifted to about 11 nm with increasing concentration of the FBFPB. These results indicating that the interaction between the FBFPB and BSA and the fluorescence quenching of BSA by FBFPB was the result of the formation of BSA–FBFPB complex [25]. These results confirmed that the quenching was mainly a static quenching process.

3.5. Molecular docking

Molecular docking technique is an attractive scaffold to understand the ligand–protein interactions which can substantiate our experimental results. Descriptions of the 3-D structure of crystalline albumin have revealed that BSA is made up of three homologous domains (I, II, and III): I (residues 1–183), II (184–376), III (377–583), each containing two subdomains (A and B) that assemble to form heart shaped molecule (Fig. 7), which are divided into

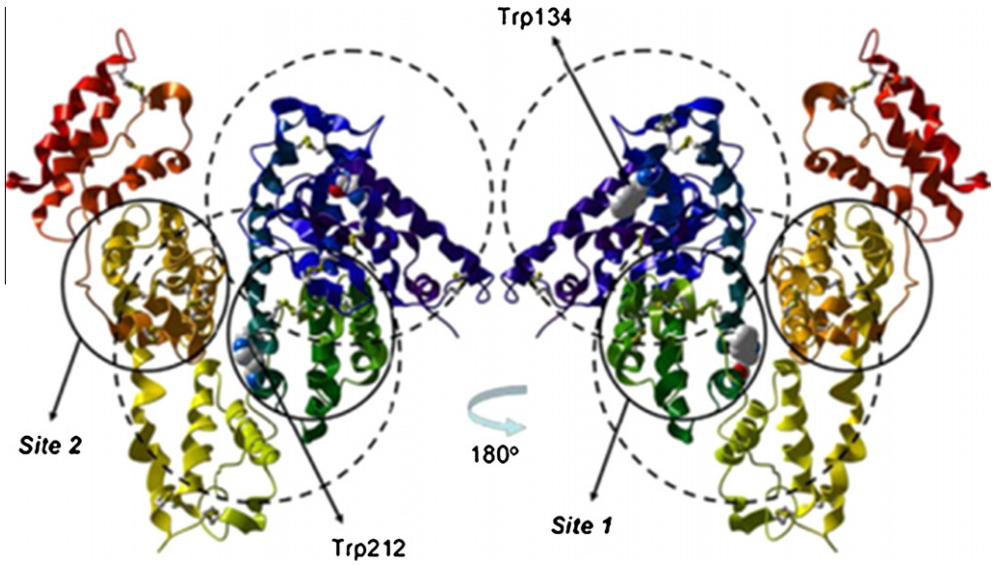

Fig. 7. Modeling of X-ray crystallographic structure of BSA (PDB ID: 1AO6). The domains and subdomains were displayed with different color, the every subdomain and classical binding site were marked in the corresponding location. (For interpretation of the references to colour in this figure legend, the reader is referred to the web version of this article.)

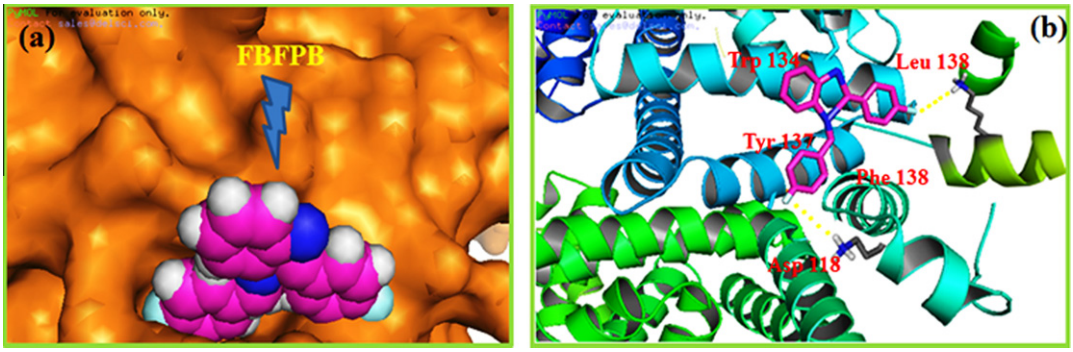

Fig. 8. (a) Molecular docked model of FBFPB (sphere representation) located within the hydrophobic pocket of BSA. (b) The hydrogen bond interaction (yellow dashed line) between FBFPB (stick) and BSA (cartoon). (For interpretation of the references to colour in this figure legend, the reader is referred to the web version of this article.)

nine loops by 17 disulphide bonds, each one formed by six helices, and its secondary structure is dominated by α-helix. It is suggested that the principal regions of ligand binding to BSA are located in hydrophobic cavities in subdomains IIA and IIIA, and one tryptophan residues (Trp-212) of BSA is in subdomain IIA [26]. There is a large hydrophobic cavity in subdomain IIA to accommodate the drug molecule, which play an important role in absorption, metabolism, and transportation of BSA. The best energy ranked results (Fig. 8a) revealed that FBFPB was located within subdomain IIA hydrophobic cavity in close proximity to positively charge hydrophobic residues, such as Asp-118, Asp-129, Leu-138, Phe-126, Phe-133, Pro-117, Trp-134 and Tyr-137, suggesting the existence of hydrophobic interaction between them. Hence, this finding provides a good structural basis to explain the efficient fluorescence quenching of BSA emission in the presence of the FBFPB. Furthermore, there are also a number of specific electrostatic interactions and hydrogen bonds, because several ionic and polar residues in the proximity of the ligand play an important role in stabilizing the molecule via H–bonds and electrostatic interactions. As shown in Fig. 8b, there are hydrogen bond interactions between the fluorine atoms of FBFPB and Leu-138 and Asp-118 residues of BSA. These results suggest that the formation of hydrogen bonds decreased the hydrophilicity and increased the hydrophobicity to keep the FBFPB–BSA system stable. On the other hand, the amino acid residues with benzene ring can match that of the structure of FBFPB in space in order to confirm the conformation of the molecule. On the other hand, the amino acid residues with a benzene ring can match that of the FBFPB in space in order to firm the conformation of the complex stability. Therefore it can be concluded that the interaction between the FBFPB and BSA was dominated by hydrophobic forces as well as hydrogen bonds, correlated well with the binding mode observed by fluorescence quenching mechanism of BSA in presence of FBFPB.

4. Conclusion

In this paper, we investigated the interaction of 1-(4-Fluorobenzyl)-2-(4-fluorophenyl)-1H-benzo[d]imidazole (FBFPB) with bovine serum albumin (BSA) by fluorescence spectroscopy and UV–vis absorption spectroscopy. The experimental results of fluorescence showed that the quenching of BSA by FBFPB is a result of the formation of BSA–FBFPB complex. A synchronous fluorescence spectrum shows the interaction of the FBFPB with BSA affects the conformation of tyrosine residues micro-region. Molecular docking studies confirms the interaction between the FBFPB and BSA.

Acknowledgments

One of the authors Prof. J. Jayabharathi is thankful to DST [No. SR/S1/IC-73/2010], UGC (F. No. 36-21/2008 (SR)) and DRDO (NRB-213/MAT/10-11) for providing funds to this research study. K. Jayamoorthy is thankful to DST (No. SR/S1/IC-73/2010) for providing fellowship.

References

[1] W.S. Hung, J.T. Lin, C.H. Chien, Y.T. Tao, S.S. Sun, Y.S. Wen, Highly phosphorescent bis-cyclometallated iridium complexes containing benzoimidazole-based ligands, Chem. Mater 16 (2004) 2480–2488.
[2] K. Nakashima, Lophine derivatives as versatile analytical tools, Biomed. Chromatogr. 17 (2003) 83–95.
[3] A. Mallick, S.C. Bera, S. Maiti, N. Chattopadhya, Fluorometric investigation of interaction of 3-acetyl-4-oxo-6,7-dihydro-12H indolo-[2,3-a] quinolizine with bovine serum albumin, Biophys. Chem. 112 (2004) 9–14.
[4] U. Kragh-Hansen, Molecular aspects of ligand binding to serum albumin, Pharmacol Rev. 33 (1) (1981) 17–53.
[5] Y. Li, W.Y. He, H.X. Liu, X.J. Yao, Z.D. Hu, Daidzein, Daidzein interaction with human serum albumin studied using optical spectroscopy and molecular modeling methods, J. Mol. Struct. 831 (1–3) (2007) 44–50.
[6] P. Sevilla, J.M. Rivas, F. Garcia-Blanco, J.V. Garcia-Ramos, S. Sanchez-Cortes, Identification of the anti tumoral drug emodin binding sites in bovine serum albumin by spectroscopic methods, Biochim. Biophys. Acta 1774 (11) (2007) 1359–1369.
[7] J. Jayabharathi, V. Thanikachalam, M. Venkatesh Perumal, Studies on interaction between an imidazole derivative and bovine serum by spectral methods, Spectrochim. Acta A 95 (2012) 622–626.
[8] J. Jayabharathi, V. Thanikachalam, K. Jayamoorthy, N. Srinivasan, Binding interaction of 1-(4-methybenzyl)-2-p-tolyl-1h-benzo[d]imidazole with bovine serum albumin, Spectrochim. Acta A 93 (2012) 180–184.
[9] J. Jayabharathi, V. Thanikachalam, M. Venkatesh Perumal, A study on the binding interaction between the imidazole derivative and bovine serum albumin by fluorescence spectroscopy, J. Lumin. 132 (2012) 707–712.
[10] J. Jayabharathi, V. Thanikachalam, K. Brindha Devi, M. Venkatesh Perumal, Binding interaction of bioactive imidazole with bovine serum albumin—A mechanistic investigation, Spectrochim. Acta Part A 83 (2011) 587–591.
[11] D. Mustard, D.W. Ritchie, Docking essential dynamics eigenstructures, proteins: struct, Funct. Bioinf. 60 (2005) 269–274.
[12] J. Jayabharathi, V. Thanikachalam, K. Jayamoorthy, Antioxidant benzimidazole bind bovine serum albumin, J. Photochem. Photobiol. B: Biol. 115 (2012) 85–92.
[13] J. Jayabharathi, V. Thanikachalam, M. Venkatesh Perumal, N. Srinivasan, Fluorescence resonance energy transfer from a bio-active imidazole derivative 2-(1-phenyl-1H-imidazo[4,5-f][1,10]phenanthrolin-2-yl)phenol to a bioactive indoloquinolizine system, Spectrochim. Acta A 79 (2011) 236–244.
[14] J.R. Lakowicz, Principles of Fluorescence Spectroscopy, third ed., Springer Publisher, New York, 2006.
[15] H. Cao, D. Wu, H. Wang, M. Xu, Effect of the glycosylation of flavonoids on interaction with protein, Spectrochim. Acta A 73 (2009) 972–975.
[16] S.N. Timaseff, Thermodynamics of protein interactions, in: H. Pecters (Ed.), Proteins of Biological Fluids, Pergamon Press, Oxford, 1972, pp. 511–519.
[17] T. Forster, Intermolecular energy migration and fluorescence, Ann. Phys. 2 (1948) 55–75.
[18] M.M. Yang, X.L. Xi, P. Yang, Study of the interaction of cephalosporin class medicine with albumin by fluorescence enhancement and fluorescence quenching theories, Chin. J. Chem. 24 (2006) 642–648.
[19] G.Z. Chen, X.Z. Huang, J.G. Xu, Z.Z. Zheng, Z.B. Wang, Methods of Fluorescence Analysis, second ed., Science Press, Beijing, 1990.
[20] J.N. Miller, Photoluminescence and chemiluminescence methods of drug analysis, Proc. Anal. Div. Chem. Soc. 16 (1979) 203–208.
[21] Y.J. Hu, Y. Liu, W. Jiang, R.M. Zhao, S.S. Qu, Fluorometric investigation of the interaction of bovine serum albumin with surfactants and 6-mercaptopurine, J. Photochem. Photobiol. B: Biol. 80 (2005) 235–242.
[22] J.H. Tang, F. Luan, X.G. Chen, Binding analysis of glycyrrhetinic acid to human serum albumin: fluorescence spectroscopy, FTIR, and molecular modeling, Bioorg. Med. Chem. 14 (2006) 3210–3217.

[23] W.C. Abert, W.M. Gregory, G.S. Allan, The binding interaction of coomassie blue with proteins, Anal. Biochem. 213 (1993) 407–413.
[24] Y.L. Wei, J.Q. Li, C. Dong, S.M. Shuang, D.S. Liu, C.W. Huie, Investigation of the association behaviors between biliverdin and bovine serum albumin by fluorescence spectroscopy, Talanta 70 (2006) 377–382.
[25] Q. Sun, Z. Li, X. Zeng, M. Ge, D. Wang, Structures and properties of the hydrogen-bond complexes: theoretical studies for the coupling modes of the pyrazole–imidazole system, J. Mol. Struct. (Theochem) 724 (2005) 167–172.
[26] B. Bhattacharya, S. Nakka, L. Guruprasad, A. Samanta, Interaction of bovine serum albumin with dipolar molecules: fluorescence and molecular docking studies, J. Phys. Chem. B 113 (2009) 2143–2150.